Supplementary Material for: "Measurement of the Spin-Transfer-Torque Vector in Magnetic Tunnel Junctions"

Jack C. Sankey, Yong-Tao Cui, Robert A. Buhrman, Daniel C. Ralph

Cornell University, Ithaca, New York 14853, USA

Jonathan Z. Sun, John C. Slonczewski[†]

IBM T. J. Watson Research Center, Yorktown Heights, New York 10598, USA

[†]IBM RSM Emeritus

Supplementary Note 1: Derivation of the ST-FMR signal $\langle V_{\mathrm{mix}} \rangle$ (Eq. (2) in the main text)

This derivation generalizes arguments in references [S1,S2,S3] in order to consider experiments in which a finite bias is applied to the sample.

We consider only the specific geometry relevant to our experiment and define the coordinate axes as in ref. [S2]. We assume that the orientation $\hat{\boldsymbol{m}}$ of the free-layer moment undergoes small-angle precession about the $\hat{\boldsymbol{z}}$ axis, that the plane of the sample is the $\hat{\boldsymbol{y}}$-$\hat{\boldsymbol{z}}$ plane, that easy axis of the free layer is along $\hat{\boldsymbol{y}}$, and that the orientation $\hat{\boldsymbol{M}}_{fixed}$ of the fixed-layer moment is in the plane of the sample and differs from $\hat{\boldsymbol{z}}$ by an angle θ_0 toward $\hat{\boldsymbol{y}}$. Let θ be the angle between $\hat{\boldsymbol{m}}$ and $\hat{\boldsymbol{M}}_{fixed}$. The precession of the free layer in response to the current $I(t) = I + \delta I(t)$ (where $\delta I(t) = I_{RF}\,\mathrm{Re}\left(e^{i\omega t}\right)$) can be characterized by the transverse components $m_x(t) = \mathrm{Re}\left(m_x e^{i\omega t}\right)$ and $m_y(t) = \mathrm{Re}\left(m_y e^{i\omega t}\right)$. Because of the large magnetic anisotropy of the thin film sample, $|m_x| << |m_y|$ and changes in the angle θ during precession are to good approximation $\delta\theta(t) = -\mathrm{Re}\left(m_y e^{i\omega t}\right)$.

The time-dependent voltage *V(t)* across the sample will depend on the instantaneous value of the current and θ. The DC voltage signal produced by rectification in ST-FMR can be calculated by Taylor-expanding *V(t)* to 2nd order and taking the time average over one precession period

$$\langle V_{\text{mix}} \rangle = \frac{1}{2}\frac{\partial^2 V}{\partial I^2}\left\langle (\delta I(t))^2 \right\rangle + \frac{\partial^2 V}{\partial I \partial \theta}\left\langle (\delta I(t))(\delta\theta(t)) \right\rangle + \frac{1}{2}\frac{\partial^2 V}{\partial \theta^2}\left\langle (\delta\theta(t))^2 \right\rangle. \quad \text{(S1)}$$

Here $\langle\ \rangle$ denotes the time average. With this expression, we assume that voltage signals due to spin pumping [S3] are negligible in tunnel junctions. Using $\delta\theta(t) = -\text{Re}\left(m_y e^{i\omega t}\right)$, Eq. (S1) can be expressed

$$\langle V_{\text{mix}} \rangle = \frac{1}{4}\frac{\partial^2 V}{\partial I^2} I_{RF}^2 - \frac{1}{2}\frac{\partial^2 V}{\partial I \partial \theta} I_{RF}\,\text{Re}\left(m_y\right) + \frac{1}{4}\frac{\partial^2 V}{\partial \theta^2}\left|m_y\right|^2. \quad \text{(S2)}$$

We calculate the precession angle m_y from the Landau-Lifshitz-Gilbert equation of motion in the macrospin approximation, with the addition of spin-transfer-torque terms transverse to the free-layer moment.

$$\frac{d\hat{\mathbf{m}}}{dt} = -\gamma \hat{\mathbf{m}} \times \vec{\mathbf{H}}_{\text{eff}} + \alpha \hat{\mathbf{m}} \times \frac{d\hat{\boldsymbol{m}}}{dt} - \gamma \frac{\tau_{\parallel}(I,\theta)}{M_s Vol}\hat{\boldsymbol{y}} - \gamma \frac{\tau_{\perp}(I,\theta)}{M_s Vol}\hat{\boldsymbol{x}}, \quad \text{(S3)}$$

where γ is the magnitude of the gyromagnetic ratio, α is the Gilbert damping coefficient, and $M_s Vol$ is the total magnetic moment of the free layer. For our specific experimental geometry, $\vec{\boldsymbol{H}}_{\text{eff}} = -N_x M_{\text{eff}}\hat{\boldsymbol{x}} - N_y M_{\text{eff}}\hat{\boldsymbol{y}}$ with $N_x = 4\pi + (H/M_{\text{eff}})$ and $N_y = (H - H_{\text{anis}})/M_{\text{eff}}$. Here H is the external magnetic field along $\hat{z}$, $4\pi M_{\text{eff}}$ is the effective anisotropy perpendicular to the sample plane, and H_{anis} denotes the strength of anisotropy within the easy plane. (If the precession axis is not along a high-symmetry direction like $\hat{\boldsymbol{z}}$, there are additional off-diagonal demagnetization terms in $\vec{\boldsymbol{H}}_{\text{eff}}$ that will

make the general expression for the ST-FMR signal more complicated than the one that we derive here [S2].)

For small RF excitation currents, the spin-torque terms can be Taylor-expanded,

$$\tau_{\parallel}(I,\theta) = \tau_{\parallel}^{0} + \frac{\partial \tau_{\parallel}}{\partial I}\delta I(t) + \frac{\partial \tau_{\parallel}}{\partial \theta}\delta\theta(t),\ \ \tau_{\perp}(I,\theta) = \tau_{\perp}^{0} + \frac{\partial \tau_{\perp}}{\partial I}\delta I(t) + \frac{\partial \tau_{\perp}}{\partial \theta}\delta\theta(t). \qquad \text{(S4)}$$

We have used a different sign convention than ref. [S2], so that the variables η_1 and η_2 in ref. [S2] correspond at zero bias to $\eta_1 = -\frac{2e}{\hbar \sin(\theta)}\frac{\partial \tau_{\parallel}}{\partial I} \equiv -\zeta_{\parallel}$ and $\eta_2 = -\frac{2e}{\hbar \sin(\theta)}\frac{\partial \tau_{\perp}}{\partial I} \equiv -\zeta_{\perp}$ in our notation.

The oscillatory terms in the equation of motion are

$$\begin{aligned} i\omega m_x &= -m_y\left(\gamma N_y M_{\text{eff}} + i\alpha\omega\right) - \frac{\gamma}{M_s Vol}\left(\frac{\partial \tau_{\perp}}{\partial I} I_{RF} - \frac{\partial \tau_{\perp}}{\partial \theta} m_y\right). \\ i\omega m_y &= m_x\left(\gamma N_x M_{\text{eff}} + i\alpha\omega\right) - \frac{\gamma}{M_s Vol}\left(\frac{\partial \tau_{\parallel}}{\partial I} I_{RF} - \frac{\partial \tau_{\parallel}}{\partial \theta} m_y\right). \end{aligned} \qquad \text{(S5)}$$

At this stage, we have neglected the influence of the DC spin-torque terms in shifting the precession axis of the free layer away from $\hat{\boldsymbol{z}}$. For the bias range of our experiment, this is a very small effect. Solving these equations for m_y to lowest order in the damping coefficient α we have

$$m_y = \frac{\gamma I_{RF}}{2M_s Vol}\frac{1}{(\omega - \omega_m - i\sigma)}\left[i\frac{\partial \tau_{\parallel}}{\partial I} + \frac{\gamma N_x M_{\text{eff}}}{\omega_m}\frac{\partial \tau_{\perp}}{\partial I}\right]. \qquad \text{(S6)}$$

Here, the resonant precession frequency is $\omega_m = \gamma M_{\text{eff}}\sqrt{N_x N_y}$ and the linewidth is

$$\sigma = \frac{\alpha\gamma M_{\text{eff}}\left(N_x + N_y\right)}{2} - \frac{\gamma}{2M_s Vol}\frac{\partial \tau_{\parallel}}{\partial \theta}. \qquad \text{(S7)}$$

In the expression for the resonant precession frequency, we have neglected a correction $\propto \partial\tau_{\perp}/\partial\theta$ that is negligible for our experiment. The small shifts in the resonant frequency

that we measure as a function of bias (see Supplementary Figure S1c) may be associated with micromagnetic phenomena that go beyond our macrospin approximation [4].

If we define $S(\omega) = 1/\{1 + [(\omega - \omega_m)/\sigma]^2\}$, $A(\omega) = [(\omega - \omega_m)/\sigma]S(\omega)$, and $\Omega_\perp = \gamma N_x M_{\text{eff}}/\omega_m$, and substitute Eq. (S6) into Eq. (S2), we reach:

$$\begin{aligned}\langle V_{\text{mix}} \rangle = &\frac{1}{4}\frac{\partial^2 V}{\partial I^2} I_{RF}^2 + \frac{1}{2}\frac{\partial^2 V}{\partial\theta\partial I}\frac{\hbar\gamma\sin\theta}{4e\, M_s Vol\ \sigma} I_{RF}^2 \left(\zeta_\parallel S(\omega) - \zeta_\perp \Omega_\perp A(\omega)\right) \\ &+ \frac{1}{4}\frac{\partial^2 V}{\partial\theta^2}\left(\frac{\hbar\gamma\sin\theta}{4e\, M_s Vol\ \sigma}\right)^2 I_{RF}^2 \left(\zeta_\parallel^2 + \zeta_\perp^2 \Omega_\perp^2\right) S(\omega).\end{aligned} \tag{S8}$$

The final term in Eq. (S8) represents a DC voltage generated by a change in the average low-frequency resistance due to magnetic precession. This term should be approximately an odd function of bias, and we estimate that it is small in the bias range we explore. It may be the explanation for the small slope in the dependence of $d\tau_\parallel/dV$ vs. bias that we subtract off in Fig. 3b of the main paper; however we find that the dominant contribution to the frequency-symmetric component of the ST-FMR signal is symmetric in bias. For these reasons we do not consider this final term in the main paper. The first two terms on the right in Eq. (S8) are then identical to Eq. (2) in the main text.

Equation (6) in the main text follows from Eq. (S7) after using $\omega_m = \gamma M_{\text{eff}}\sqrt{N_x N_y}$ and assuming that $\tau_\parallel(I,\theta) \propto \sin(\theta)$.

Supplementary Note 2: Details on the calibration of I_{RF}^2

The calibration of I_{RF}^2 is performed in two steps: (1) a flatness correction and (2) accounting for the bias dependence of the sample impedance. The flatness correction ensures that the microwave current within the sample I_{RF} does not vary with frequency.

We apply an external magnetic field H with magnitude chosen so that all ST-FMR resonances have frequencies higher than the range of interest, and then measure the ST-FMR background signal as a function of frequency for a fixed DC bias ($|I|$ > 10 μA). Due to circuit resonances and losses, this background signal may vary as the frequency is changed. At the same time, we determine $\partial^2 V/\partial I^2$ by measuring $\partial V/\partial I$ versus I with low-frequency lock-in techniques and then differentiating numerically. We can then determine the variations of I_{RF}^2 with frequency using the formula for the non-resonant background:

$$\left\langle V_{\text{background}} \right\rangle = \frac{1}{4}\frac{\partial^2 V}{\partial I^2} I_{RF}^2 . \tag{S9}$$

We input this information to the microwave source, and employ its flatness-correction option to modulate the output signal so that the final microwave current coupled to the sample no longer varies with frequency.

(2) After step (1), I_{RF} is leveled vs. frequency and its magnitude can be determined for one set of values I_0 and H_0. However, because the sample impedance varies as a function of I and H, we must also determine how I_{RF} varies as these quantities are changed. In order to do this accurately even at points where $\partial^2 V/\partial I^2$ is near zero, we calculate $I_{RF}(I,H)$ by taking into account how variations in dI/dV alter the termination of the transmission line, assuming that the impedance looking out from the junction is 50 Ω:

$$I_{RF}(I,H) = I_{RF}(I_0,H_0)\left[\frac{dV}{dI}(I_0,H_0)+50\,\Omega\right]\Big/\left[\frac{dV}{dI}(I,H)+50\,\Omega\right]. \tag{S10}$$

In practice, we generally determine $I_{RF}(I_0, H_0)$ using Eq. (S9) together with the value of the non-resonant background at one choice of I_0 for each value of magnetic field, and

then employ (S10) to find the full *I* dependence.

Supplementary Figure S2 shows that this procedure successfully reproduces the measured non-resonant background signal as a function of I_0, using as input the bias dependence of *dV/dI* measured at low frequency. This demonstrates that there are no high-frequency phenomena which cause the background signal to deviate significantly from the simple rectification signal caused by non-linearities in the low-frequency current-voltage curve. Supplementary Figure S3 shows the typical change in I_{RF} as described by Eq. (S10).

Supplementary Note 3: Regarding possible alternative mechanisms for the antisymmetric Lorentzian component of the ST-FMR signal

Kovalev et al. [S2] and Kupfershmidt et al. [S3] have noted that a component of the ST-FMR signal that is antisymmetric in frequency relative to the center frequency can arise if the precession axis of the free layer moment is tilted away from the sample plane and not along any of the principle axes of the magnetic anisotropy. In principle, this mechanism could explain an observation of an antisymmetric ST-FMR signal that varies linearly with DC current *I*, because the in-plane component of spin-transfer torque from *I* will cause the equilibrium orientation of the free-layer moment to move out-of-plane (until the torque from the demagnetization field balances the in-plane spin-transfer-torque). However, when evaluating this mechanism quantitatively, we find that it predicts an antisymmetric component 50 times smaller than we measure.

In principle, heating might affect the ST-FMR measurements through several mechanisms. Here we consider only whether a heating effect might be able to explain

our observation that the ST-FMR signal contains a perpendicular component with an antisymmetric Lorentzian lineshape, whose magnitude depends approximately linearly on I (*i.e.*, we consider heating as an alternative mechanism to the out-of-plane torkance discussed in the main paper.) If Ohmic heating is the dominant source of heating, then the sample temperature may have an RF component proportional to $dT(t) \sim R\,(I + I_{RF}(t))^2 \sim 2RI_{RF}I\cos(\omega t + \delta_T)$ (after subtracting the constant contribution $\propto RI^2$ and assuming $I > I_{RF}$), where δ_T is a possible phase lag. If heating changes the resistance of the sample, this would give an additional contribution to the resonant part of the ST-FMR signal of the form $\langle V_{\mathrm{mix}} \rangle \propto \frac{\partial^2 V}{\partial\theta\partial T}\langle(\delta\theta(t))(\delta T(t))\rangle \propto \frac{\partial^2 V}{\partial\theta\partial T} I_{RF} I \mathrm{Re}\left(m_y e^{-i\delta_T}\right)$. However, since $\partial^2 V/\partial\theta\partial T$ in this expression is proportional to I at low bias, the lowest-order contribution to the ST-FMR signal from this mechanism is proportional to I^2, so that it cannot explain the linear dependence of the asymmetric component on I observed experimentally.

An antisymmetric-in-frequency ST-FMR signal linear in I could result if the Peltier effect, rather than Ohmic heating, were the dominant heating mechanism. However, our differential conductance measurements do not show a large asymmetry with respect to bias that would be expected if this were the case. A resonant signal linear in I could also result if the dominant consequence of heating were not to change the resistance, but to apply a torque to $\hat{m}$ by changing the demagnetization or dipole field. We expect that this last mechanisms might be significant if the free layer were tilted partially out of the sample plane, but we estimate that it is insignificant for our measurements in which the free-layer moment is in plane and aligned within a few degrees of the symmetry axis $\hat{z}$.

For these reasons, we believe it is unlikely that heating, rather than a direct out-of-plane spin-transfer torque, can explain the antisymmetric component of the ST-FMR signal that we observe.

S1. Tulapurkar, A. A. *et al*. Spin-torque diode effect in magnetic tunnel junctions. *Nature* **438**, 339-342 (2005).

S2. Kovalev, A. A., Bauer, G. E. W. & Brataas, A. Current-driven ferromagnetic resonance, mechanical torques, and rotary motion in magnetic nanostructures. *Phys. Rev. B* **75**, 014430 (2007).

S3. Kupferschmidt, J. N., Adam, S. & Brouwer, P. W. Theory of the spin-torque-driven ferromagnetic resonance in a ferromagnet/normal-metal/ferromagnet structure. *Phys. Rev. B* **74**, 134416 (2006).

S4. Polianski, M. L. & Brouwer, P. W. Current-induced transverse spin-wave instability in a thin nanomagnet. *Phys. Rev. Lett*. **93**, 026602 (2004).

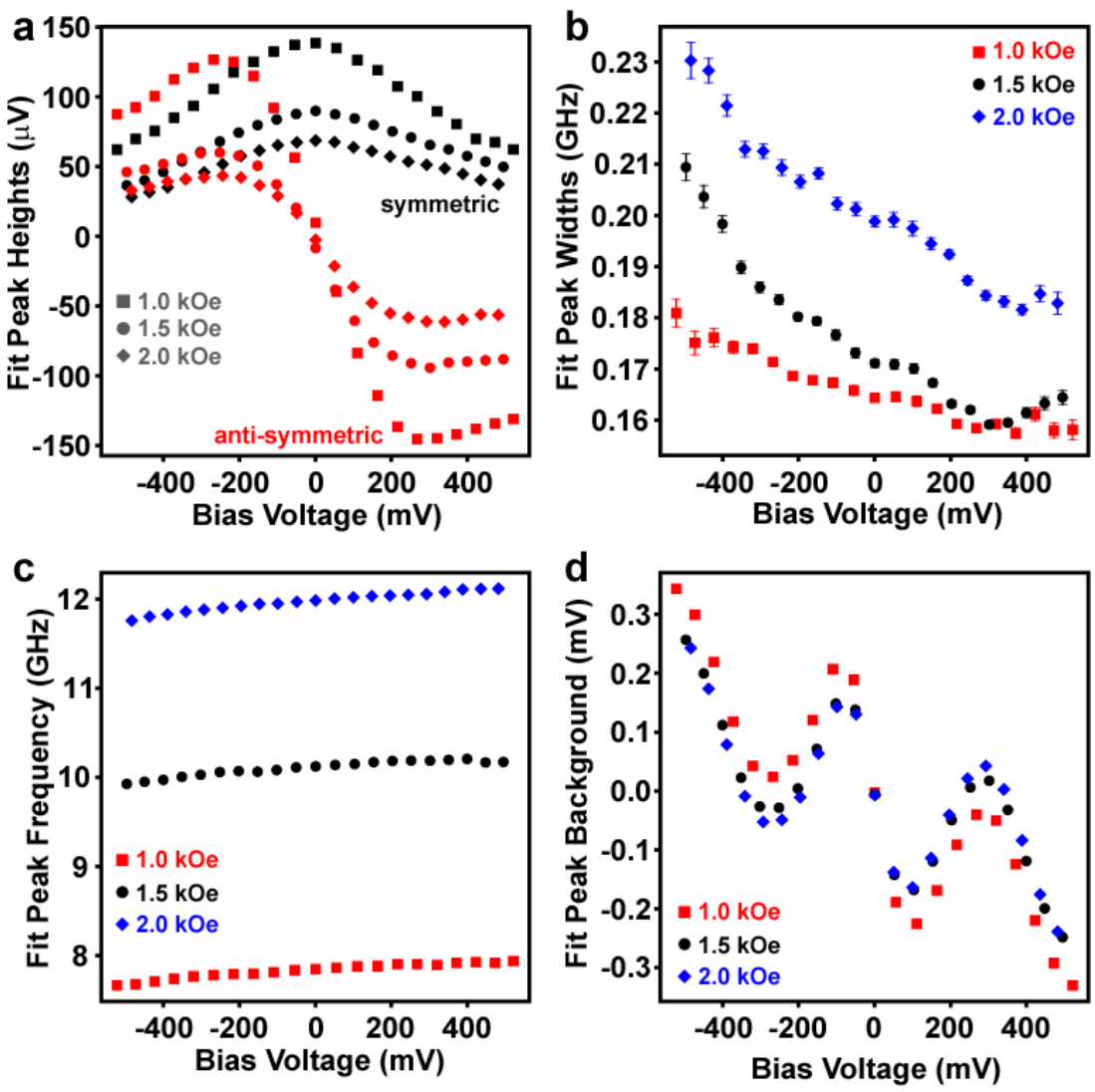

Supplementary Figure S1. Fit parameters for the ST-FMR signals at room temperature, for three values of magnetic field in the $\hat{z}$ direction and $I_{RF} \approx 12$ μA. (a) Amplitudes of the symmetric and antisymmetric Lorentzian component of each peak. (b) The linewidths $\sigma/(2\pi)$. (c) The center frequencies $\omega/(2\pi)$. (d) Non-resonant background components.

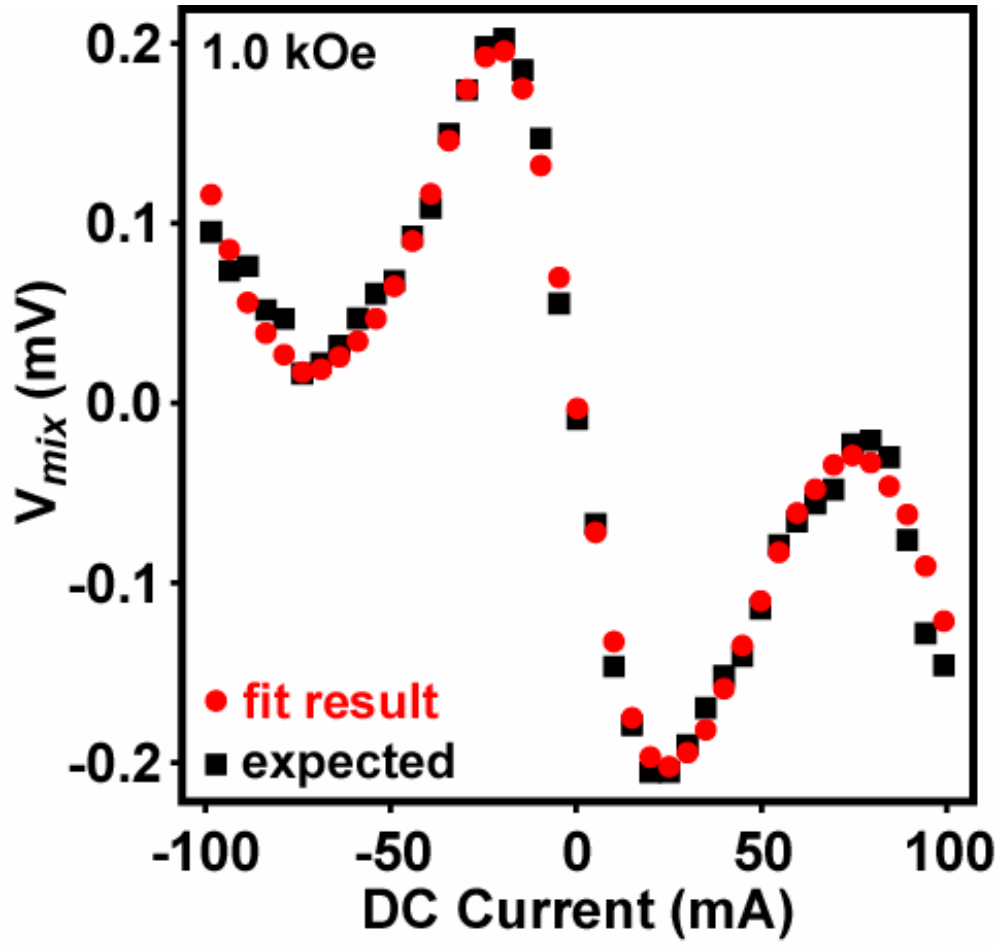

Supplementary Figure S2. Test of the calibration for I_{RF} and the non-resonant background, for H = 1.0 kOe in the $\hat{z}$ direction. Circles: Magnitude of non-resonant background measured from fits to the ST-FMR peaks. Squares: the background expected from Equations (S9) and (S10) after determining I_{RF} = 11.7 μA at I_0 = -30 μA.

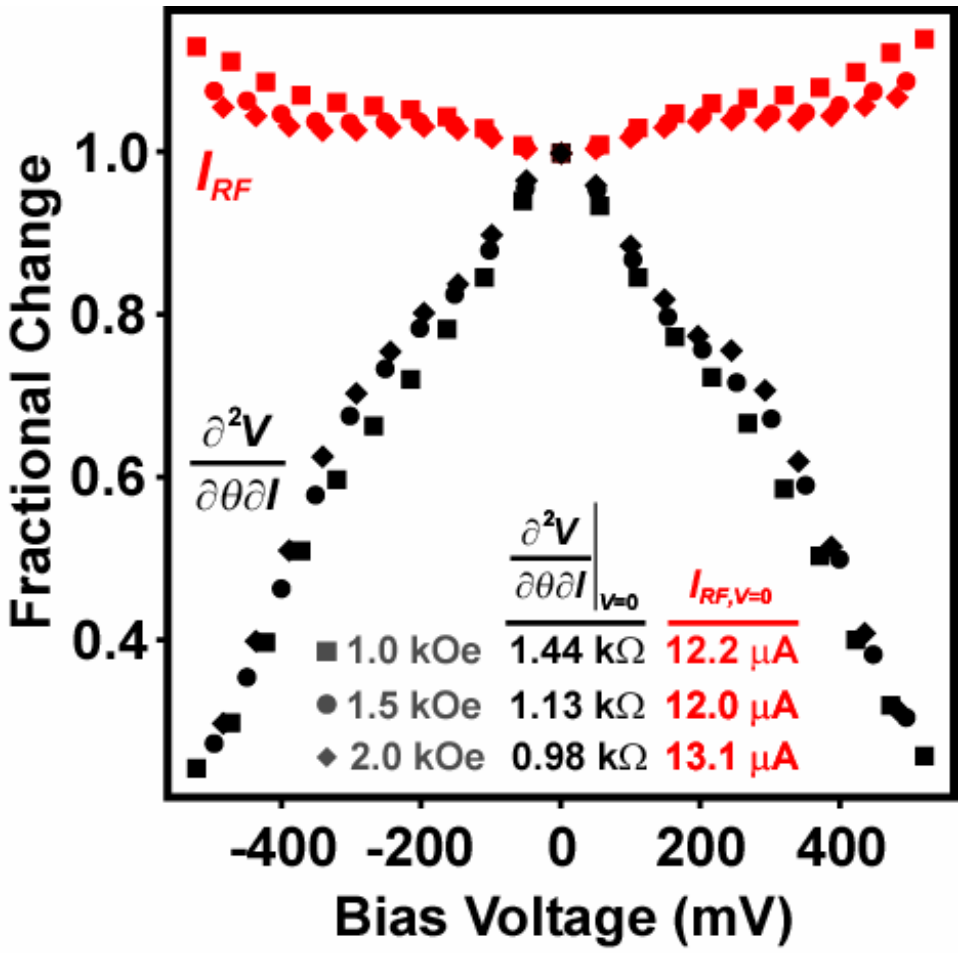

Supplementary Figure S3. Representative examples of the bias dependence of I_{RF} and $\partial^2 V/\partial\theta\partial I$ for H in the $\hat{z}$ direction. Values of I_{RF} and $\partial^2 V/\partial\theta\partial I$ at V=0 are labeled. I_{RF}^2 is determined using the procedure described above. $\partial^2 V/\partial\theta\partial I$ is determined by measuring $\partial V/\partial I$ vs. I at a sequence of magnetic fields in the $\hat{z}$ direction, by assuming that the conductance changes at zero bias are proportional to $\cos(\theta)$ and that θ depends negligibly on I, and then by performing a local linear fit to determine $\partial^2 V/\partial\theta\partial I$ for given values of I and H.

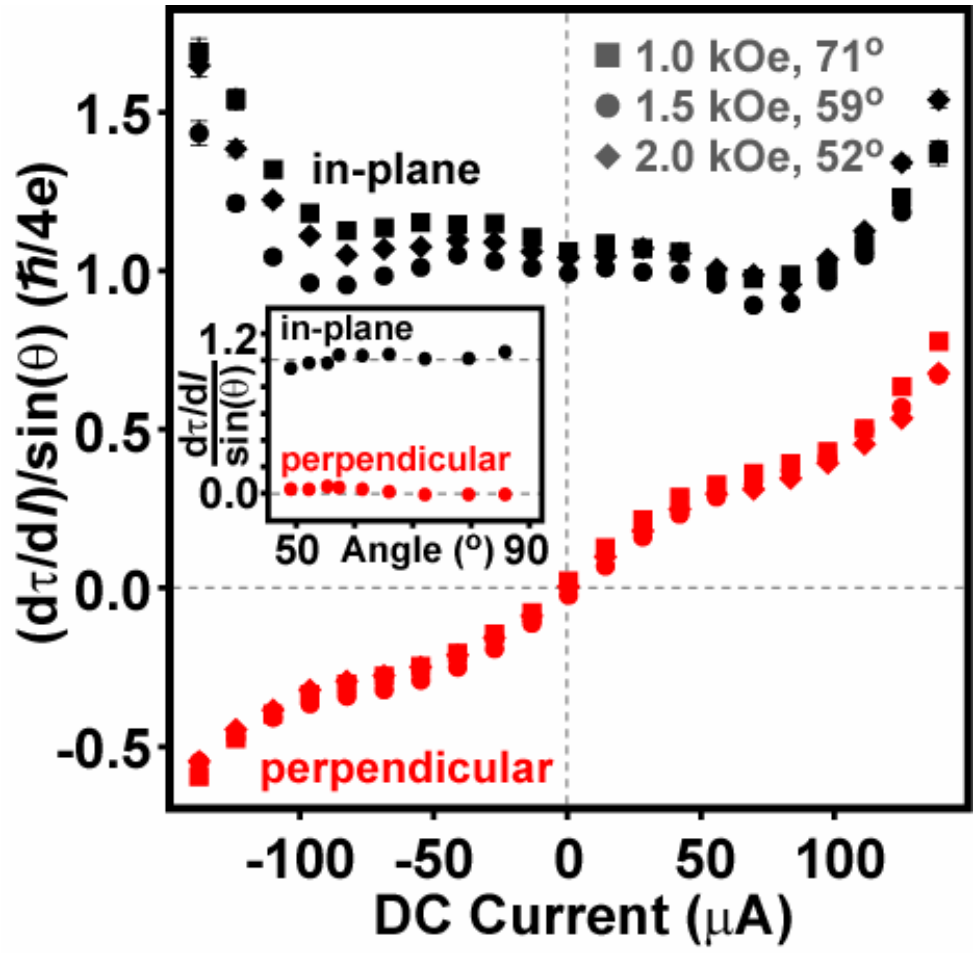

Supplementary Figure S4. Values of the in-plane and out-of plane differential torques $d\tau_{\parallel}/dI$ (black symbols) and $d\tau_{\perp}/dI$ (red symbols) vs. *I*, determined from fits to room-temperature ST-FMR spectra. The overall scale for the y-axis has an uncertainty of ~15% associated with the determination of the sample volume. (Inset) Angular dependence of the differential torques at zero bias.

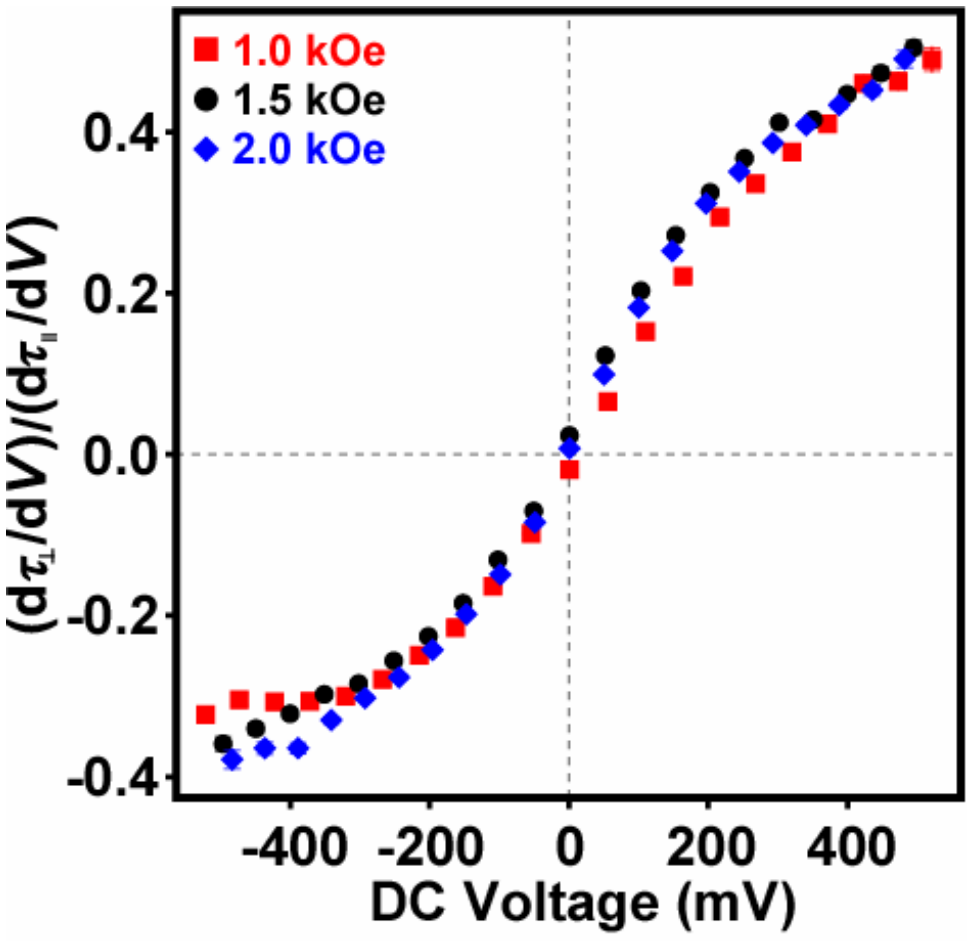

Supplementary Figure S5. Ratio of the perpendicular torkance $d\tau_{\perp}/dV$ to the in-plane torkance $d\tau_{\parallel}/dV$ as a function of bias.

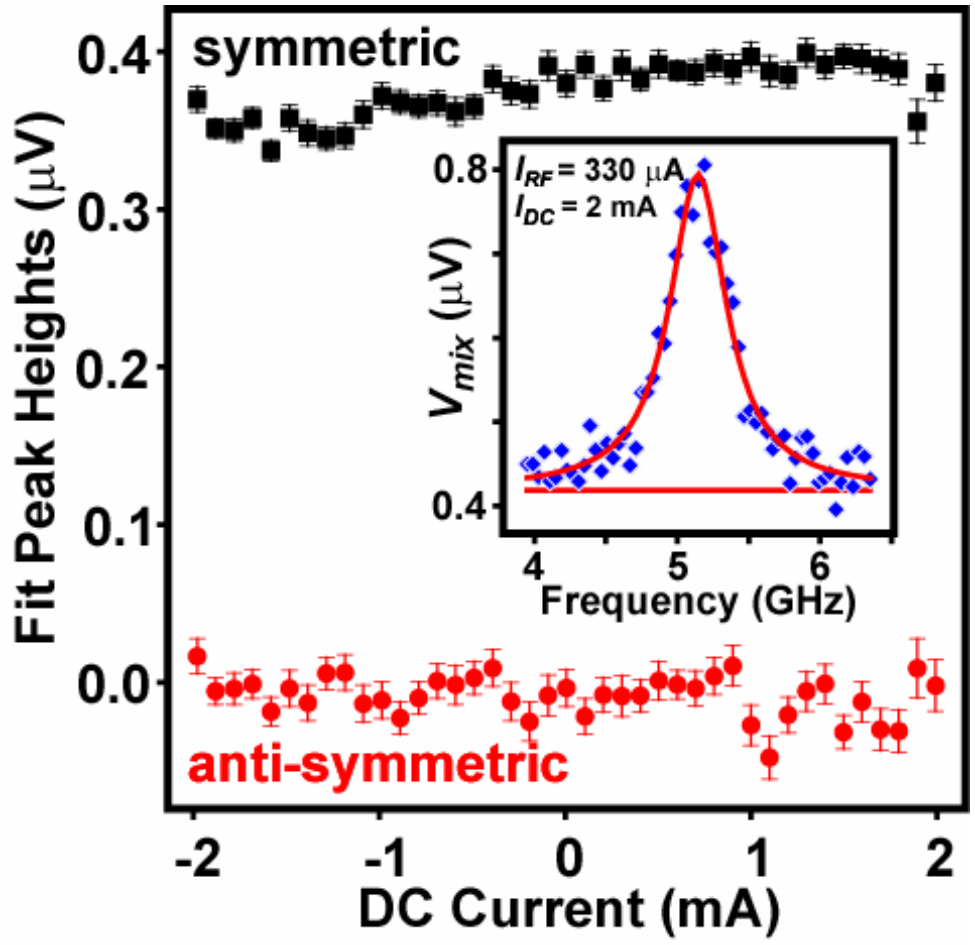

Supplementary Figure S6. ST-FMR signals for a metallic spin valve, (in nm) Py 4 / Cu 80 / IrMn 8 / Py 4 / Cu 8 / Py 4 / Cu 2 / Pt 30, with H = 560 Oe in the plane of the sample along $\hat{z}$ and with an exchange bias direction 135° from $\hat{z}$. We estimate θ=77° from the GMR. The average anti-symmetric Lorentzian component is 2 ± 3% the size of the symmetric Lorentzian component over this bias range. Accounting for the out-of-plane anisotropy $4\pi M_{\text{eff}}$ ~ 1 T in Eq. (2) of the main paper, we estimate that the ratio $\tau_{\perp} / \tau_{\parallel}$ < 1%.